Manuscript accepted for publication in Computers and Geotechnics

A BOUNDING SURFACE MECHANICAL MODEL FOR UNSATURATED CEMENTED SOILS UNDER ISOTROPIC STRESSES

Agostino Walter Bruno[1], Domenico Gallipoli[2], Mohamed Rouainia[1] and Marti Lloret-Cabot[3]

[1] School of Engineering, Newcastle University, NE1 7RU, United Kingdom

[2] Dipartimento di Ingegneria Civile, Chimica e Ambientale, University of Genoa, Italy

[3] Department of Engineering, Durham University, DH1 3LE, United Kingdom.

DATE OF SUBMISSION: 22/05/2020

NUMBER OF WORDS: 5657

NUMBER OF TABLES: 2

NUMBER OF FIGURES: 12

CORRESPONDING AUTHOR: Agostino Walter BRUNO

Newcastle University

School of Engineering – Geotechnics and Structures

Devonshire Terrace

Drummond Building, Room 2.19

NE1 7RU, Newcastle upon Tyne

United Kingdom

e-mail: **agostino.bruno@newcastle.ac.uk**

ABSTRACT:

This paper presents a model that describes the gradual yielding of unsaturated cemented soils subjected to isotropic loading. The model relies on the definition of a "cementation bonding function" which accounts for the progressive breakage of inter-granular cementation caused by loading. The combination of this cementing bonding function with the unsaturated model of Gallipoli and Bruno [1] leads to the formulation of a "cemented unified normal compression line" (CUNCL), which describes the virgin behaviour of both cemented and uncemented soils under saturated and unsaturated conditions. Gradual yielding is described by assuming that, as the soil state moves towards the CUNCL, the slope of the loading curve tends towards the slope of the CUNCL. The model describes the hysteretic variation of void ratio for both cemented and uncemented soils under saturated and unsaturated conditions by using only seven parameters, i.e. five parameters for the uncemented behaviour plus two extra parameters accounting for the effect of cementation. The model has been calibrated and validated against the experimental data of Arroyo et al. [2] demonstrating a good performance to describe the uncemented and cemented behaviour of soils under saturated and unsaturated conditions.

KEYWORDS: Cemented soils; partial saturation; bounding surface plasticity; constitutive modelling; soil yielding; soil mechanics.

INTRODUCTION

Structured soils display attributes of the transition zone from soils to rocks and are widely found in nature. The behaviour of structured soils is relevant to many civil engineering applications from mining to tunnelling and from road construction to the analysis of landslides [3-5]. A feature of structured soils is the presence of inter-particle bonding or cementation, which contributes to their strength and stiffness, and tends to progressively deteriorate as the application of loads damage the bonds between particles [6]. Many structured soil deposits are also found in the superficial ground layer and often exists in a partially saturated state. Partial saturation affects the mechanical behaviour of structured soils by causing irrecoverable degradation and softening of structured soils during loading [7]. The combined effects of partial saturation and cementation have been the object of increasing scientific interest thanks also to the development of advanced and accurate measurement techniques of suction and water content in unsaturated soils [8-9].

A number of constitutive models have been proposed to predict the mechanical behaviour of structured soils including the progressive loss of cementation under increasing stress levels [10-20]. These models consider, however, only saturated conditions and neglect the influence of partial saturation on the mechanical behaviour. In contrast, other models predict the mechanical behaviour of unsaturated soils without accounting for the effect of cementation [21-29]. Only a handful of elastoplastic models account for the combined effects of both cementation and partial saturation on the mechanical behaviour of natural soils [5-7,30-32]. These models provide, however, a limited description of mechanical hysteresis and introduce unrealistic discontinuities at the transition point between elastic and plastic states.

This paper presents a new model that describes the mechanical behaviour of natural soils in the presence of both partial saturation and cementation within the framework of bounding surface plasticity. The model predicts the progressive yielding (i.e. the development of irreversible plastic strain) of cemented soils subjected to isotropic stresses under both unsaturated and saturated conditions. The model requires a total of seven parameters, all of which have a clear physical meaning and are relatively easy to calibrate from experimental tests. Five of these seven parameters are needed to describe the uncemented behaviour of the

soil under both saturated and unsaturated conditions. Two additional parameters are instead required to describe the effect of cementation.

An important feature of the proposed model is the introduction of a single normal compression line, formulated in terms of a "cemented scaled stress", which describes the virgin behaviour of both cemented and uncemented soils under unsaturated and saturated conditions. The cemented scaled stress is based on a physical interpretation of the mechanism through which inter-granular bonds are damaged under increasing stress levels. The cemented scaled stress reduces to Terzaghi's effective stress for an uncemented saturated soil, i.e. when the degree of saturation is equal to one and at least one of the two parameters governing cementation is equal to zero. A bounding surface formulation is also proposed to predict the progressive yielding of the overconsolidated soil towards virgin conditions. The formulation differentiates between loading and unloading paths, which results in the prediction of a hysteretic behaviour consistent with experimental observations. The model has been tested for its capabilities to reproduce a series of laboratory results reported by Arroyo et al. [2], who performed isotropic loading-unloading tests on artificially cemented and uncemented soil samples under saturated and unsaturated conditions. The comparison between the simulations and experimental data confirms the good performance of the model in capturing the main features of behaviour such as the gradual yielding of the material towards an uncemented state as stress levels increase and inter-granular bonds are destroyed. The proposed framework lays the basis for a general constitutive model of unsaturated cemented soils accounting for non-isotropic stress states and incorporating the interaction between water retention and mechanical behaviour.

BOUNDING SURFACE MODEL

Bounding normally consolidated behaviour

Gallipoli and Bruno [1] proposed a unified normal compression line (UNCL) to describe the virgin loading of uncemented soils under both saturated and unsaturated conditions:

$$\log e_u = -\lambda_p \log \frac{\bar{p}}{\bar{p}_{ref}} \tag{1}$$

Eq. (1) relates the void ratio e_u of the unsaturated uncemented soil to the mean scaled stress $\bar{p}$ by means of two material parameters, $\lambda_p$and $\bar{p}_{ref}$, which are the slope and the intercept (i.e. the mean scaled stress at a reference void ratio of one) of the UNCL in the $\log e_u - \log \bar{p}$ plane. The mean scaled stress $\bar{p}$ is defined as the product of a power function of the degree of saturation S_r and the mean average skeleton stress $p' = p - u_a + S_r s$ (where $p - u_a$ is the mean net stress and $s = u_a - u_w$ is the suction with p, u_a and u_w being the mean total stress, the pore air pressure and the pore water pressure, respectively):

$$\bar{p} = S_r^{\frac{\lambda_r}{\lambda_p}} p' \tag{2}$$

In Eq. (2), the model parameter λ_r describes the effect of partial saturation on the mechanical behaviour, with larger values of λ_r corresponding to a stronger capillary bond between particles. In particular, as detailed in [1], the parameter λ_r represents the slope of the linear relationship between $\frac{e_u}{e_{u,s}}$ and S_r in a double-logarithmic plane, where $\frac{e_u}{e_{u,s}}$ is the ratio between the unsaturated uncemented void ratio e_u and the uncemented saturated void ratio $e_{u,s}$ at the same mean average skeleton stress, p'. Therefore, the parameter λ_r describes the loss of the extra porosity sustained by capillarity with increasing saturation levels. When the degree of saturation becomes one, the mean scaled stress, $\bar{p}$,reduces to Terzaghi's effective stress and the unified normal compression line (UNCL) reduces to the normal compression line (NCL) of saturated soils.

The above formulation describes the virgin behaviour of unsaturated uncemented soils and is here extended to include the effect of cementation. This is achieved by introducing a "cementation bonding function" which relates the ratio $\frac{e}{e_u}$, between the cemented void ratio e and the uncemented void ratio e_u at the same mean scaled stress $\bar{p}$, to the mean scaled stress itself according to the following monotonically decreasing function:

$$\frac{e}{e_u} = \frac{1}{\left(\frac{\bar{p}}{R + \bar{p}}\right)^{\lambda_c}} \tag{3}$$

where R and λ_c are two additional parameters whose values depend on the degree of cementation. From a physical point of view, Eq. (3) describes the progressive reduction of the extra porosity sustained by cementation as the mean scaled stress increases and inter-granular bonds are destroyed. In the limit, when the mean scaled stress tends to infinity and the inter-granular bonds are completely destroyed, Eq. (3) predicts a ratio $\frac{e}{e_u} = 1$, which means that no extra porosity is sustained by cementation. By applying logarithms to both sides of Eq. (3), one obtains the following alternative expression of the cementation bonding function:

$$\log\frac{e}{e_u} = -\lambda_c \log\left(\frac{\bar{p}}{R+\bar{p}}\right) \tag{4}$$

Inspection of Eq. (4) indicates that the parameter λ_c defines the rate with which cementation degrades as the mean scaled stress increases while the parameter R defines the value of mean scaled stress when $\frac{e}{e_u} = 2^{\lambda_c}$. The physical meaning of parameters λ_c and R is graphically illustrated in Figs. 1a and 1b, which provide two different representations of the cementation bonding function in the double-logarithmic planes $\log\frac{e}{e_u} - \log\frac{\bar{p}}{R+\bar{p}}$ and $\log\frac{e}{e_u} - \log\bar{p}$, respectively.

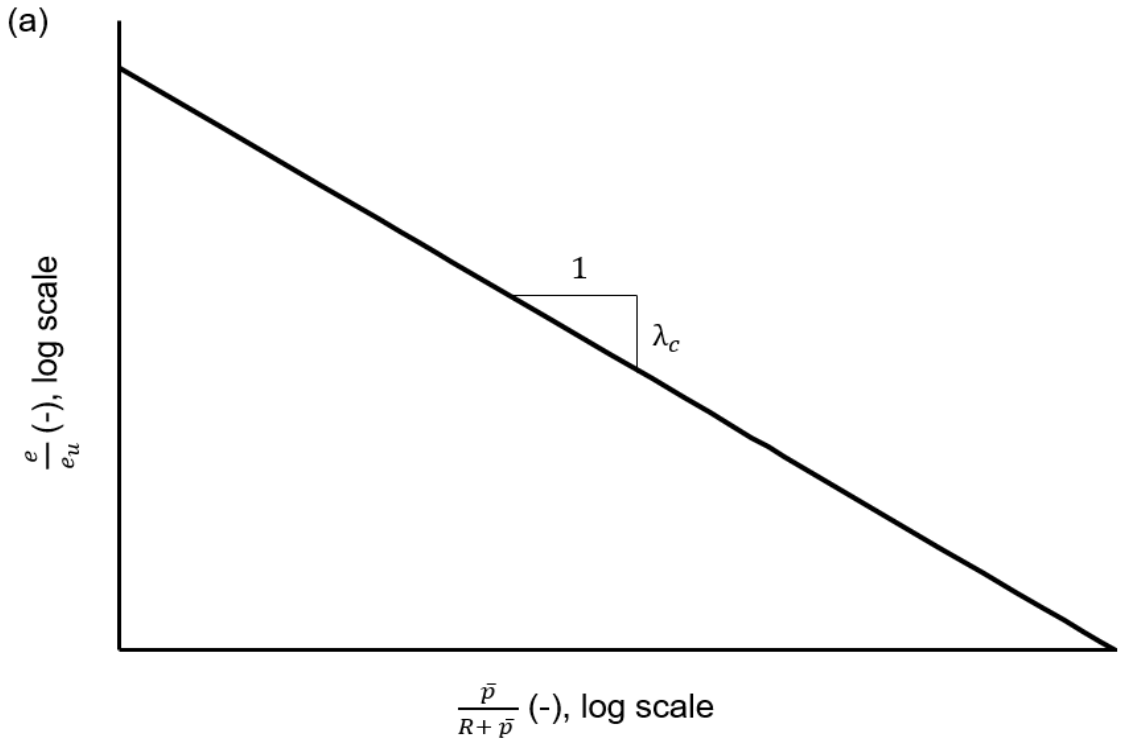

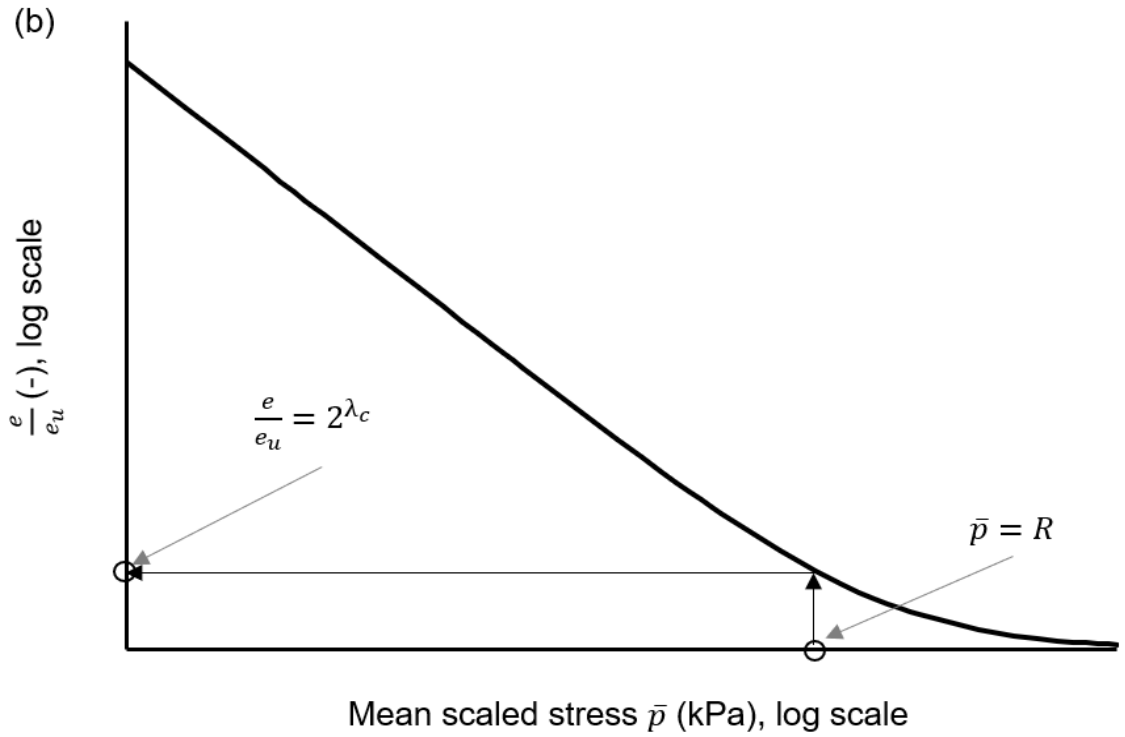

Figure 1. Cementation bonding function in the double-logarithmic planes $\log\frac{e}{e_u} - \log\frac{\bar{p}}{R+\bar{p}}$ *(a) and* $\log\frac{e}{e_u} - \log\bar{p}$ *(b)*

Combining Eqs. (1) and (4) leads to the following expression of the cemented unified normal compression line (CUNCL), which can be used to predict the variation of the cemented void ratio, e,during virgin loading under both saturated and unsaturated conditions:

$$\log e = -\lambda_p \log\left(\frac{\bar{p}}{\bar{p}_{ref}}\left(\frac{\bar{p}}{R+\bar{p}}\right)^{\frac{\lambda_c}{\lambda_p}}\right) \tag{5}$$

In Eq. (5), only two additional parameters, R and λ_c, are required to describe the cemented behaviour in addition to the three parameters $\lambda_r, \lambda_p, \bar{p}_{ref}$ which describe the uncemented behaviour of the unsaturated soil. The CUNCL reduces to the UNCL of Eq. (1) if at least one of the two cementation parameters (i.e. R and λ_c) is equal to zero.

A new constitutive variable $\bar{\bar{p}}$, called the "mean cemented scaled stress", can therefore be defined as:

$$\bar{\bar{p}} = \bar{p}\left(\frac{\bar{p}}{R+\bar{p}}\right)^{\frac{\lambda_c}{\lambda_p}} \tag{6}$$

which, once substituted in Eq. (5), results in the following simpler form of the CUNCL:

$$\log e = -\lambda_p \log\left(\frac{\bar{\bar{p}}}{\bar{\bar{p}}_{ref}}\right) \tag{7}$$

where $\bar{\bar{p}}_{ref}$ is the reference value of the mean cemented scaled stress corresponding to a void ratio of one. Note that in Eq. (7) $\bar{\bar{p}}_{ref} = \bar{p}_{ref}$ but the symbol $\bar{\bar{p}}_{ref}$ has been retained for consistency with that of the mean cemented scaled stress.

Overconsolidated behaviour

The CUNCL of Eq. (7) delimits the region of overconsolidated soil states in the $\log e - \log \bar{\bar{p}}$ plane. Inside this region, loading and unloading paths correspond to the increase and decrease of mean cemented scaled stress, respectively.

Similar to Gallipoli and Bruno [1], it is assumed that during loading the derivative of the logarithm of void ratio with respect to the logarithm of the mean cemented scaled stress (i.e. the slope of the loading path in the $\log e - \log \bar{\bar{p}}$ plane) changes monotonically towards the derivative (i.e. the slope) of the CUNCL as this is approached. This condition is mathematically expressed as:

$$\frac{d \log e}{d \log \bar{\bar{p}}} = -\lambda_p \left(\frac{\bar{\bar{p}}}{\bar{\bar{p}}_i}\right)^{\gamma} \tag{8}$$

where the slope of the loading path is equal to the slope of the normal compression line λ_p reduced by a power factor $\left(\frac{\bar{\bar{p}}}{\bar{\bar{p}}_i}\right)^{\gamma}$ smaller than one. The argument $\frac{\bar{\bar{p}}}{\bar{\bar{p}}_i}$ is always smaller than one as it is the ratio between the current value of mean cemented scaled stress $\bar{\bar{p}}$ and its image value $\bar{\bar{p}}_i$ on the CUNCL at the same void ratio (Fig. 2). Moreover, the ratio $\frac{\bar{\bar{p}}}{\bar{\bar{p}}_i}$ tends to one as the soil state approaches the CUNCL, which ensures a smooth transition towards the CUNCL as shown in Fig. 2. The exponent γ is instead a positive material parameter that controls the rate with which the loading path tends towards the CUNCL.

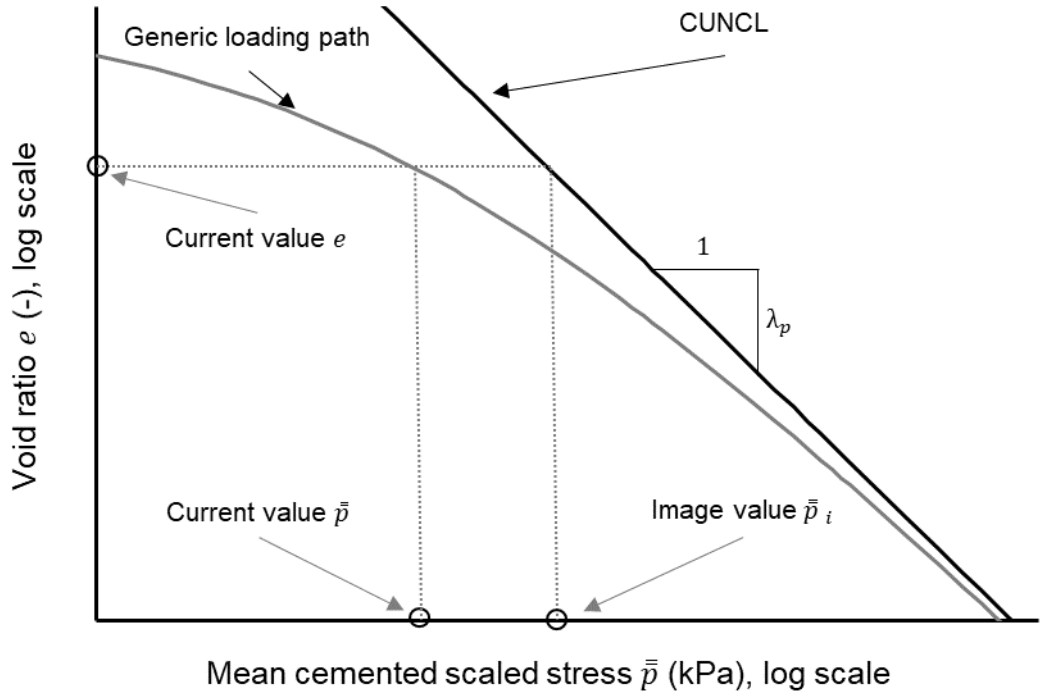

Figure 2. Generic loading path and bounding CUNCL in the double-logarithmic plane $\log e - \log \bar{\bar{p}}$

The image value of the mean cemented scaled stress is obtained from Eq. (7) as:

$$\bar{\bar{p}}_i = \frac{\bar{\bar{p}}_{ref}}{e^{\frac{1}{\lambda_p}}} \tag{9}$$

Substituting Eq. (9) into Eq. (8) leads to the following differential equation:

$$\frac{d \log e}{d \log \bar{\bar{p}}} = -\lambda_p \left(\frac{\bar{\bar{p}} e^{\frac{1}{\lambda_p}}}{\bar{\bar{p}}_{ref}} \right)^{\gamma} \tag{10}$$

which is analytically solved to yield the following closed form expression of the void ratio which is valid for all loading curves:

$$e = \left[\left(\frac{\bar{\bar{p}}}{\bar{\bar{p}}_{ref}} \right)^{\gamma} + C_L \right]^{-\frac{\lambda_p}{\gamma}} \tag{11}$$

In Eq. (11), C_L is a constant of integration that is unique to each loading curve and is calculated by imposing a suitable boundary condition, i.e. by introducing a pair of known values of void ratio, e_0, and mean cemented scaled stress, $\bar{\bar{p}}_0$, as:

$$C_L = e_0^{-\frac{\gamma}{\lambda_p}} - \left(\frac{\bar{\bar{p}}_0}{\bar{\bar{p}}_{ref}}\right)^{\gamma} \tag{12}$$

According to the definition of mean cemented scaled stress (see Eqs. (6) and (2)), a loading path may, therefore, be produced by the increases of net stress, degree of saturation or suction. This means that inter-granular cementation may be damaged not only by external loads but also by changes of degree of saturation and suction.

During unloading, the model assumes that the derivative of the logarithm of void ratio with respect to the logarithm of the cemented scaled stress is constant and equal to $-\kappa$:

$$\frac{d\log e}{d\log \bar{\bar{p}}} = -\kappa \tag{13}$$

This implies that all unloading paths are linear in the $\log e - \log \bar{\bar{p}}$ plane and the swelling coefficient, κ is unaffected by the degradation of inter-granular cementation. This is consistent with the work of Gallipoli and Bruno [1], who assumed that the swelling coefficient, κ is unaffected by capillary bonding. The assumption of a constant swelling coefficient, κ is justified by the fact that the effects of cementation and capillarity are already included in the definition of the scaled stress and is also supported by experimental evidence.

Similar to loading paths, Eq. (13) can be integrated in a closed form giving:

$$e = \frac{C_U}{\bar{\bar{p}}^{\kappa}} \tag{14}$$

where C_U is a constant of integration that is unique to each unloading curve and is calculated by imposing a suitable boundary condition, i.e. by substituting known values of void ratio e_0 and mean cemented scaled stress $\bar{\bar{p}}_0$ in Eq. (14) as:

$$C_U = e_0 \bar{\bar{p}}_0^{\kappa} \tag{15}$$

In summary, the proposed model requires a total of five parameters, λ_p, λ_r, $\bar{\bar{p}}_{ref}$, γ and κ, to predict the smooth hysteretic variation of void ratio in unsaturated uncemented soils and two extra parameters, R and λ_c, to describe the effect of inter-granular cementation.

MODEL CALIBRATION

Model parameters were calibrated against two sets of isotropic loading-unloading tests performed by Arroyo et al. [2] on samples of silty sand compacted at the same water content of 13%. In the first set of tests, samples were compacted at a dry density of 1684 kg/m^3, either uncemented or with 2% and 7% of cement. In the second set of tests, samples were compacted at a lower dry density of 1526 kg/m^3, either uncemented or with 4% of cement. All unsaturated tests were performed at constant water content without measurement of suction. Knowledge of suction is however necessary in the proposed model to calculate the mean cemented scaled stress and was therefore estimated from the measured values of water content and void ratio using the soil-water retention model of Gallipoli et al. [33]. This retention model uniquely relates the degree of saturation S_r to the void ratio e and suction s by means of the following equation:

$$S_r = \left[\frac{1}{1 + (\Phi\, s\, e^{\psi})^n}\right]^m \tag{16a}$$

which is recast in terms of gravimetric water content w as:

$$w(\%) = \frac{e}{G_s}\left[\frac{1}{1 + (\Phi\, s\, e^{\psi})^n}\right]^m \times 100 \tag{16b}$$

where Φ, ψ, m and n are four model parameters and G_s is the specific gravity of the soil equal to 2.72 for the material tested by Arroyo et al. [2]. This relatively simple retention law was preferred to a more sophisticated hysteretic model (e.g. [34]) due to the availability of only drying tests. There is, in principle, no difficulty in extending the developed model to account for the effects of pore size on capillarity through a suitable retention law (e.g. [35,36]), but this level of complexity was considered outside the

scope of the present work. The retention model of Eq. (16) was calibrated against data from drying tests on samples with different proportions of cement equal to 0% (uncemented), 2%, 4% and 7% [2]. The retention behaviour was measured, at different values of void ratio, up to a suction level of 1000 kPa by means of Mercury Intrusion Porosimetry (MIP) tests (Fig. 3). For suctions beyond 1000 kPa, only one drying curve at a single value of void ratio was measured, for each cementation level, by means of psychrometer tests. This is enough because, when suction is large, the variation of water content becomes independent of void ratio as observed by Barrera [37], Lloret et al. [38] and Salager et al. [39], among others. The data of Arroyo et al. [2] also show that the drying curves at different values of void ratio tend to merge as suction increases (Fig. 3). Note that Arroyo et al. [2] assumed that soil porosity did not vary during MIP tests and that each drying curve obtained from these tests corresponds to a constant void ratio, an assumption that is retained in the present work.

Four different sets of retention parameters were selected, one set for each cementation level, by best-fitting Eq. (16b) to the drying tests in Figs. 3. As suggested by Gallipoli [40] and Gallipoli et al. [34], the product of the three parameters ψ, m and n was fixed to one to ensure that the retention behaviour becomes independent of void ratio over the high suction range. The choice of distinct sets of parameters for different percentages of added cement accounts for the effect of cementation on the retention behaviour and is also consistent with the subsequent calibration of the mechanical model. It should be noted that at the highest void ratio the retention model does not capture well the sudden drop of water content in correspondence of the air entry value of the soil (Fig. 3). This is, however, irrelevant to the subsequent mechanical predictions as all loading-unloading tests considered in this work have been performed at relatively high levels of suction, well above the air entry value of the soil.

The above retention law of Eq. (16b) was then used to estimate the suction values corresponding to experimental measurements of water content and void ratio during the subsequent calibration and validation of the mechanical model.

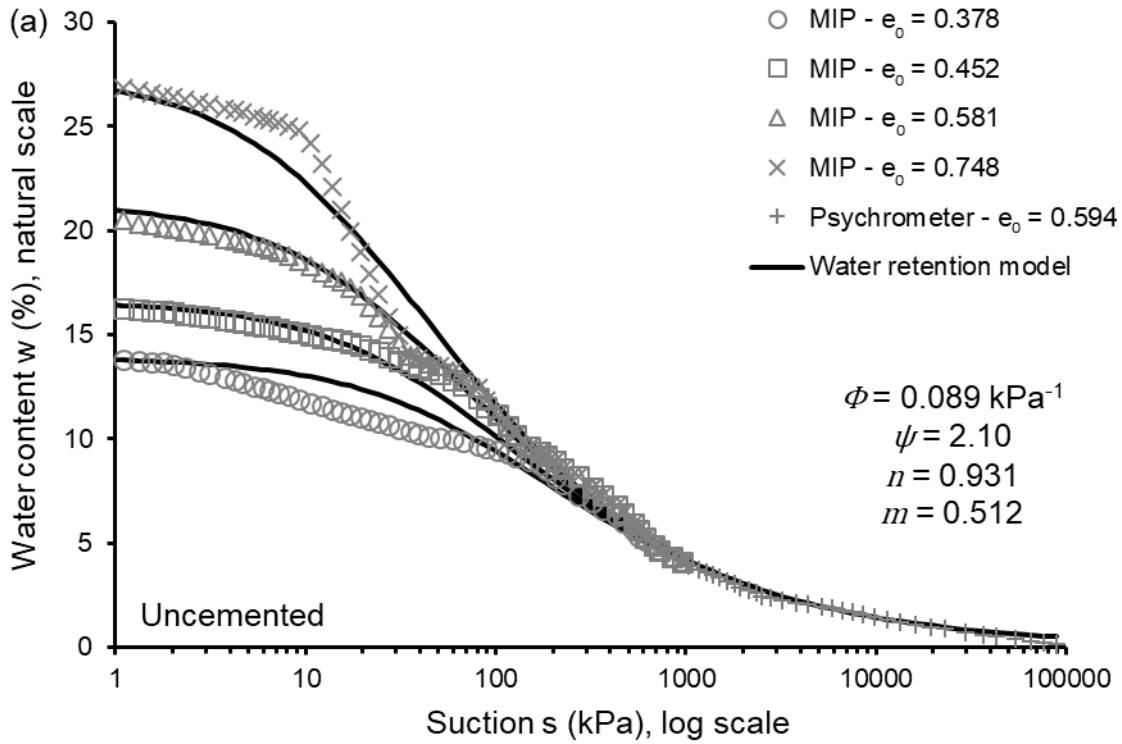
(a)
Water content w (%), natural scale
Suction s (kPa), log scale
MIP - e0 = 0.378
MIP - e0 = 0.452
MIP - e0 = 0.581
MIP - e0 = 0.748
Psychrometer - e0 = 0.594
Water retention model
Φ = 0.089 kPa-1
ψ = 2.10
n = 0.931
m = 0.512
Uncemented

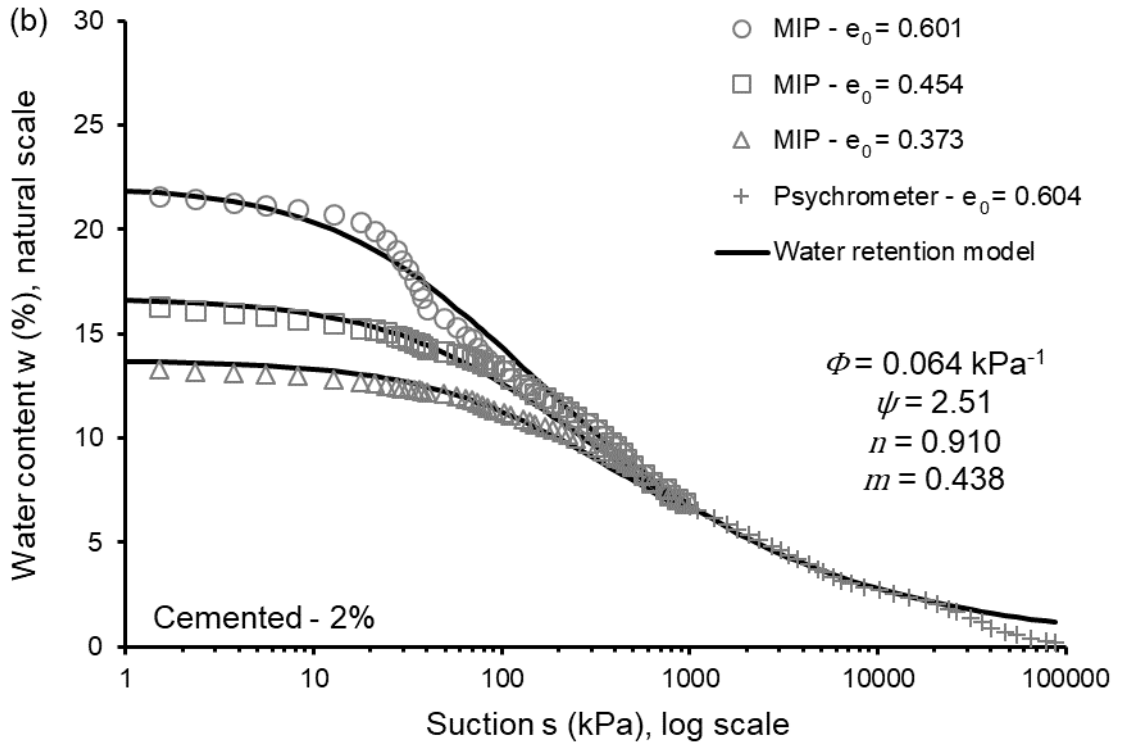
(b)
Water content w (%), natural scale
Suction s (kPa), log scale
MIP - e0 = 0.601
MIP - e0 = 0.454
MIP - e0 = 0.373
Psychrometer - e0 = 0.604
Water retention model
Φ = 0.064 kPa-1
ψ = 2.51
n = 0.910
m = 0.438
Cemented - 2%

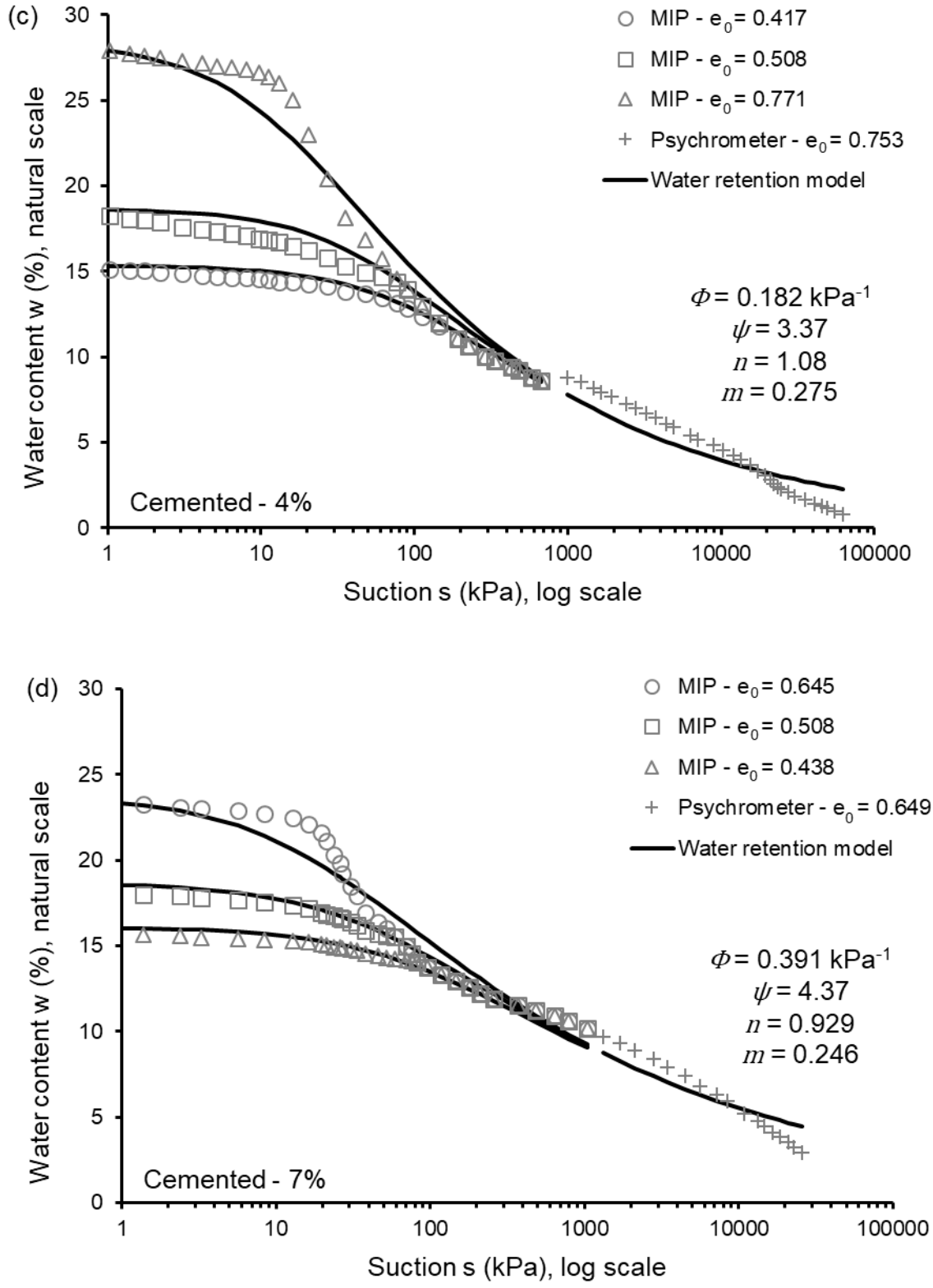

Figure 3. Calibration of water retention behaviour of samples with proportions of cement equal to 0%, i.e. uncemented (a), 2% (b), 4% (c) and 7% (d)

The proposed mechanical model was calibrated in two stages to highlight the different physical meaning of the five parameters governing the uncemented behaviour in both saturated and unsaturated states ($\lambda_p, \bar{\bar{p}}_{ref}, \lambda_r, \gamma$ and k) and the two parameters describing the effect of cementation (R and λ_c). In the first stage, the uncemented parameters $\lambda_p, \bar{\bar{p}}_{ref}, \lambda_r, \gamma$ and k were selected by best-fitting Eqs. (11) and (14) to loading-unloading tests on unsaturated uncemented samples, with parameters R and λ_c set to zero inside the expression of the mean cemented scaled stress. In the second stage, the previously selected uncemented parameters were maintained constant while the values of R and λ_c were calibrated by best-fitting Eqs. (11) and (14) to loading-unloading tests on cemented samples under saturated and unsaturated conditions. This two-stage calibration process emphasizes the distinct effects of model parameters on material behaviour but an alternative procedure, where all parameters are simultaneously selected from tests on unsaturated cemented samples, could have also been employed.

The uncemented parameters $\lambda_p, \bar{\bar{p}}_{ref}, \lambda_r, \gamma$ and k were calibrated against two isotropic loading-unloading tests on unsaturated uncemented samples (Fig. 4). The two samples were compacted at the same water content of 13% under slightly different loads to produce two distinct dry densities of 1684 kg/m^3 and 1526 kg/m^3, respectively. The identical compaction water content suggests the existence of a similar material fabric and justifies the assumption of the same uncemented parameters for both density levels. In Fig. 4, the higher density sample (triangular markers) was initially dried to a water content of 4.4% and subsequently loaded at constant water content. The lower density sample (circular markers) was, instead, initially dried to a water content of 8.0% and subsequently loaded at constant water content. Fig. 4 also reports the values of degree of saturation measured at the beginning and end of each loading/unloading path, together with the corresponding values of suction calculated by Eq. (16b) from the measurements of water content and void ratio. Inspection of Fig. 4 indicates a good agreement between simulations and experiments, which confirms the ability of the model to predict the void ratio of the uncemented soil along stress paths involving large variations of mean net stress, degree of saturation and suction. This is, however, an expected result because, when R and λ_c are set to zero, the present model reduces to that of Gallipoli and Bruno [1] for unsaturated uncemented soils, which has already been validated against multiple sets of experimental data. Table 1

summarizes the values of the five uncemented parameters, which are identical for both density levels as discussed earlier.

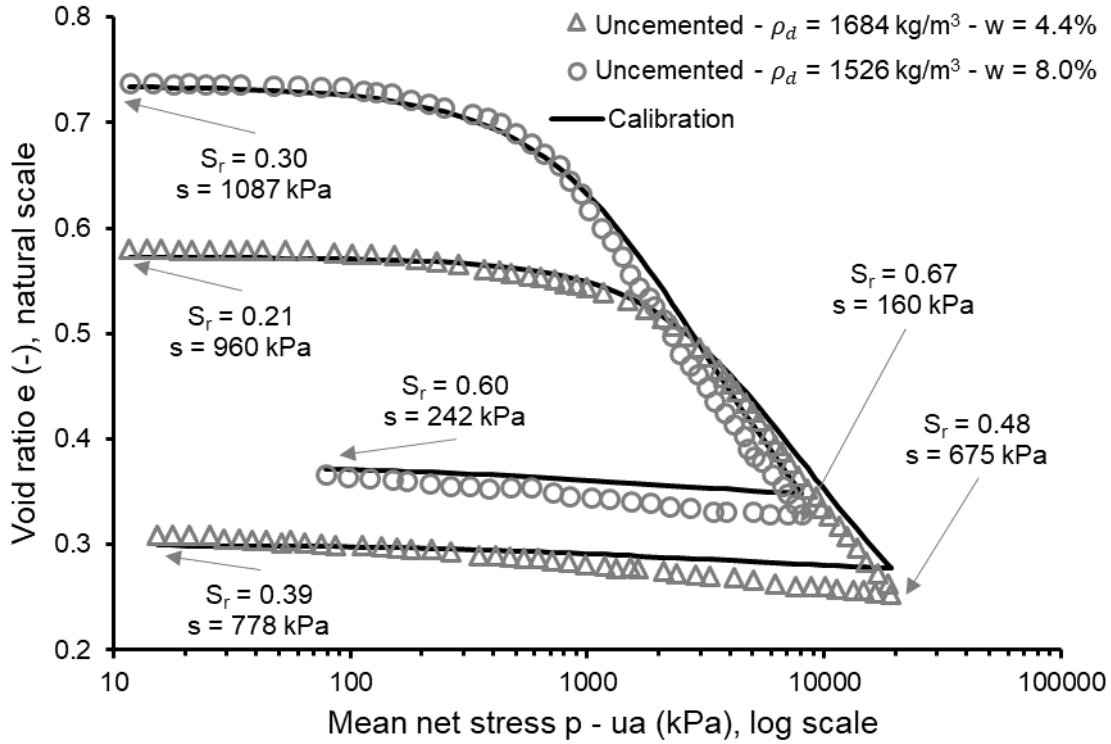

Figure 4. Calibration of the uncemented behaviour of samples compacted at the dry densities of 1526 kg/m³ and 1684 kg/m³

In the second stage, the two parameters governing the cemented behaviour, i.e. R and λ_c, were estimated as the best-fitting of isotropic loading-unloading tests on cemented samples under both saturated and unsaturated conditions. Results are plotted in Figs. 5, 6 and 7 for the three cementation levels of 2%, 4% and 7%, respectively. The samples stabilised with 2% and 7% of cement were compacted at a dry density of 1684 kg/m³, while the samples stabilised with 4% of cement were compacted at a lower dry density of 1526 kg/m³. Also, all samples were compacted at the same water content of 13% under slightly different loads to achieve the distinct density levels.

Two loading-unloading tests were simultaneously best-fitted for each cementation level, namely one test under saturated conditions (Figs. 5a, 6a and 7a) and one test under unsaturated conditions (Figs. 5b, 6b and 7b). Given the saturated state of the material, Figs. 5a, 6a and 7a also show the initial values of water content,

w_0, which changed during the subsequent loading-unloading paths. Similarly, for the unsaturated tests, Figs. 5b, 6b and 7b show the initial values of water content, w, which were kept constant throughout the subsequent loading-unloading paths. Figs. 5b, 6b and 7b also report the values of degree of saturation measured at the beginning and end of each loading/unloading path, along with the corresponding values of suction calculated using Eq. (16b) from the measurements of water content and void ratio. Note that, in the best-fit of the above tests on cemented samples, the five uncemented parameters were maintained constant and equal to the values estimated from the first calibration stage. Inspection of Figs. 5, 6 and 7 indicates a good agreement between simulations and experiments for all cementation levels under both saturated and unsaturated conditions. This confirms the ability of the model to predict the progressive decay of cementation with increasing load levels and the associated variation of void ratio.

Table 1 summarizes the values of the parameters governing the behaviour of the unsaturated cemented soil. The parameters R and λ_c depend on the initial degree of cementation and therefore differ for the three percentages of added cement.

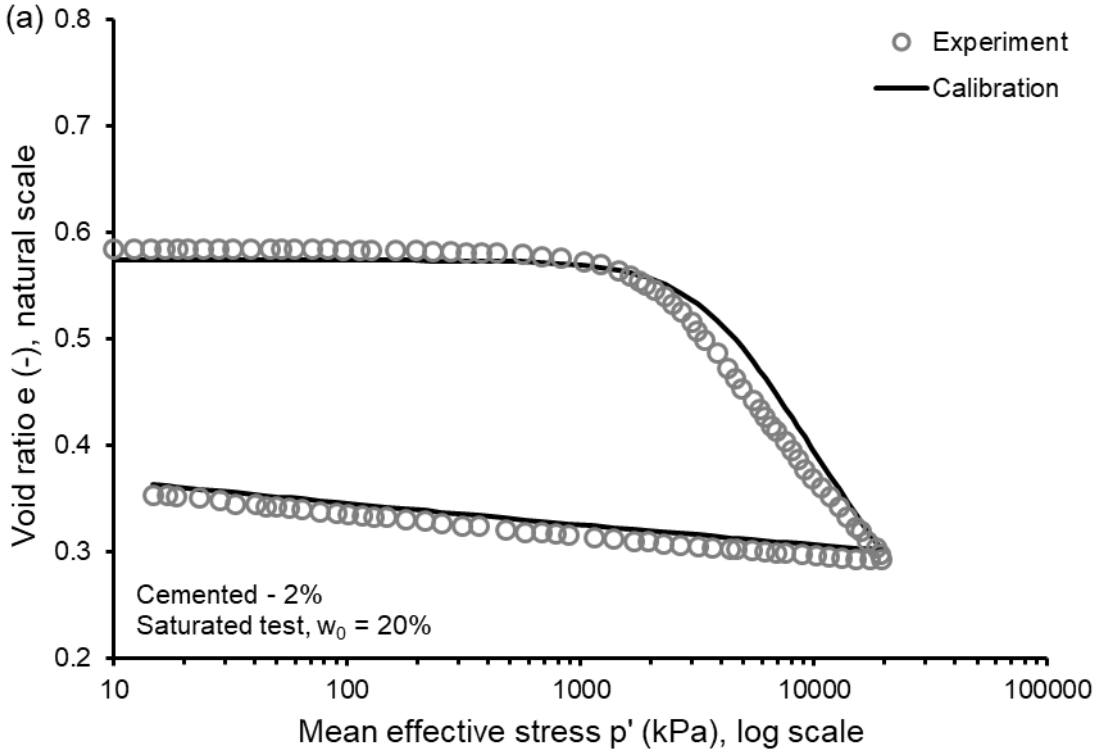

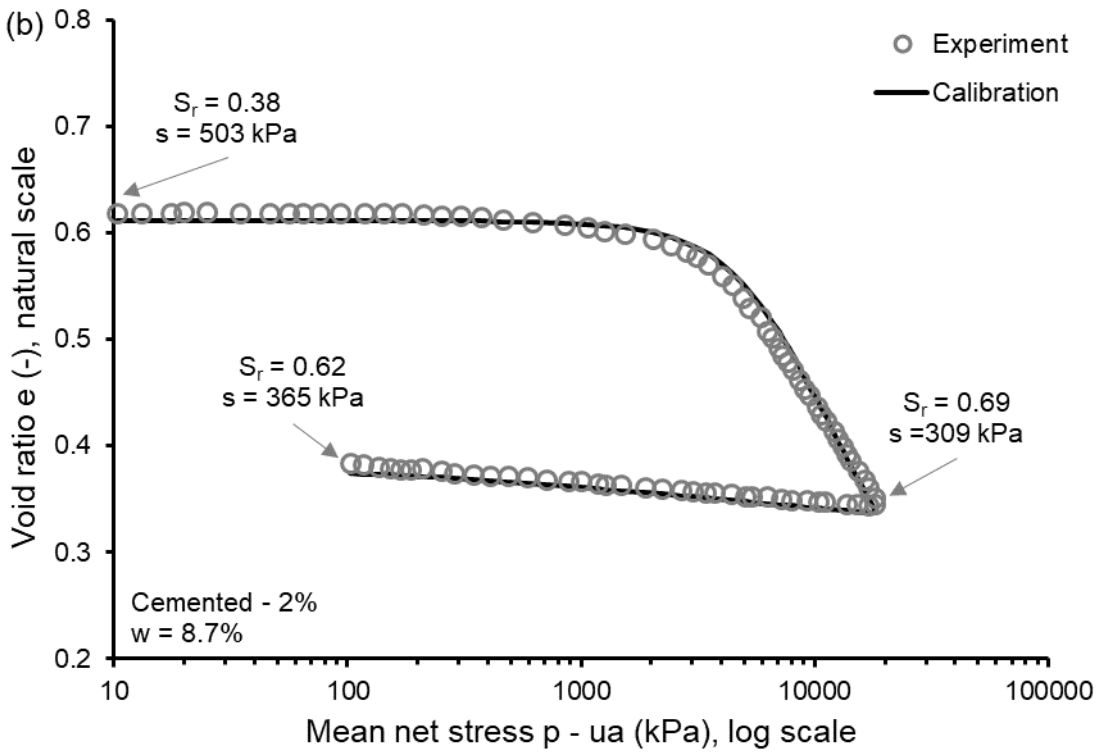

Figure 5. Calibration of cemented behavior of samples with 2% of cement under saturated conditions (a) and unsaturated conditions (b)

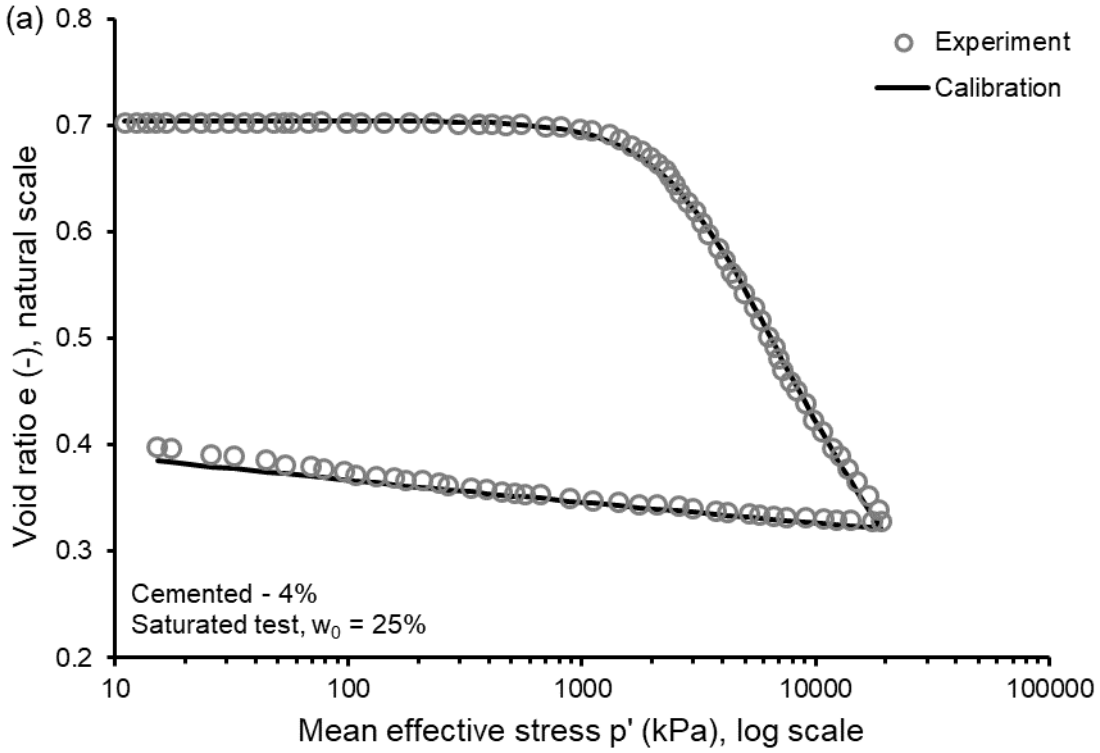

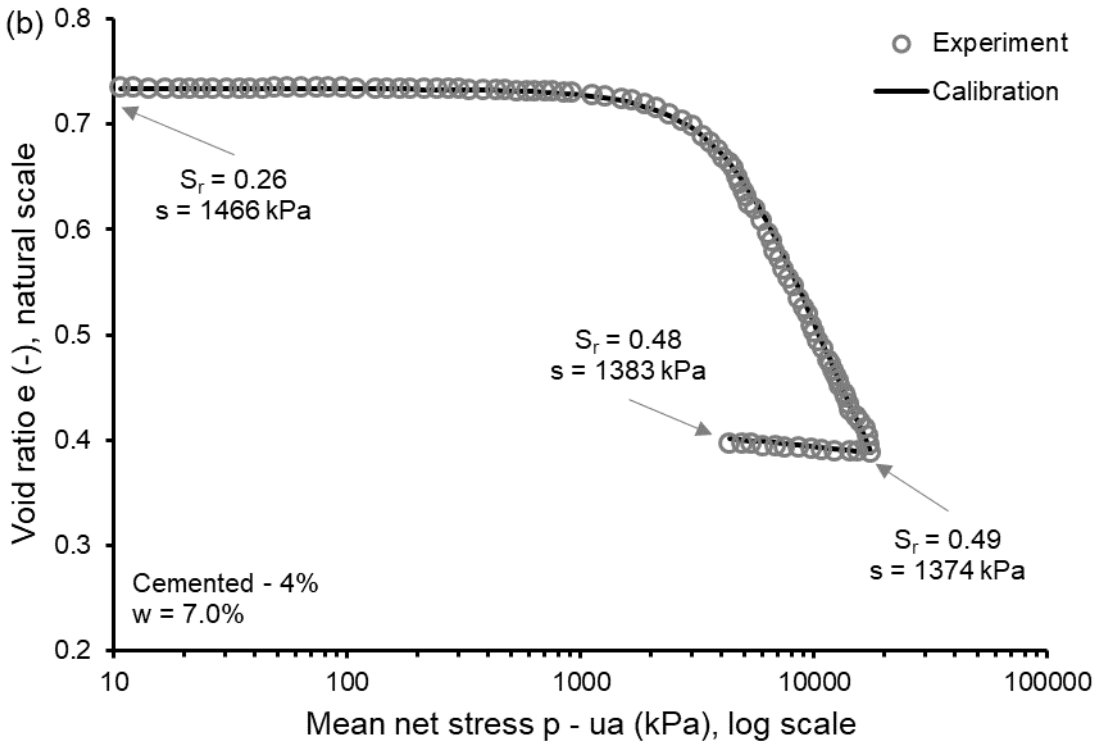

Figure 6. Calibration of cemented behavior of samples with 4% of cement under saturated conditions (a) and unsaturated conditions (b)

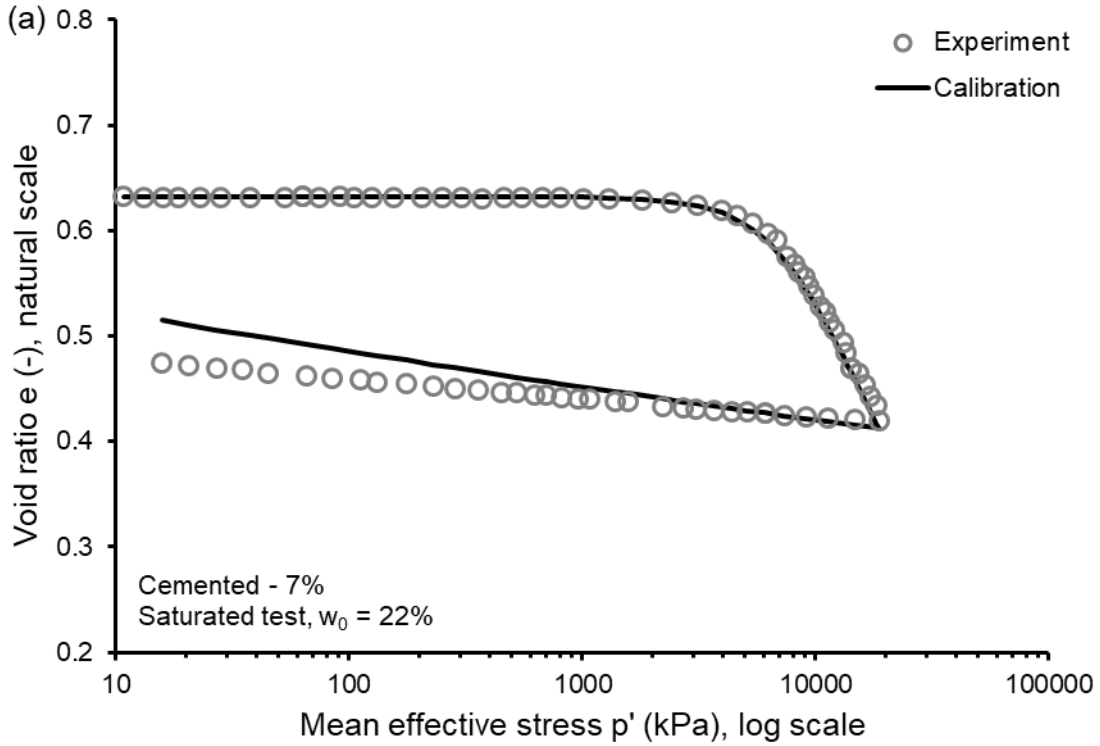

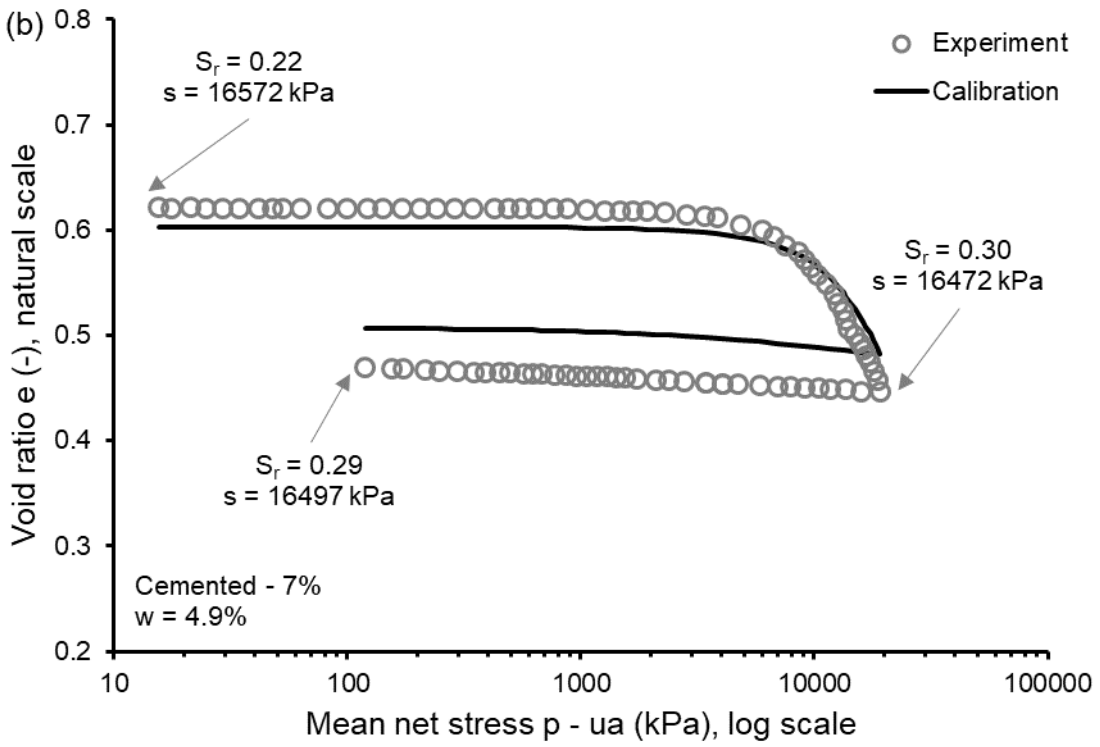

Figure 7. Calibration of cemented behavior of samples with 7% of cement under saturated conditions (a) and unsaturated conditions (b)

Table 1. Values of model parameters

Uncemented behaviour parameters	λ_p	0.327		
	$\bar{\bar{p}}_{ref}$	266 kPa		
	λ_r	0.177		
	γ	1.49		
	κ	0.018		
		Percentage of added cement		
		2%	4%	7%
Cemented behaviour parameters	λ_c	0.147	0.134	0.245
	R	67227 kPa	124670 kPa	151221 kPa

In the above interpolations, the constant of integration C_L of the initial loading path was treated as an additional fitting variable of Eq. (11) like Gallipoli et al. [34]. Conversely, during the subsequent unloading path, the constant of integration C_U of Eq. (14) was calculated by imposing the continuity of the predicted curve at the reversal point, i.e. by imposing that the start of the unloading path coincides with the end of the loading path. Note also that experimental values of the degree of saturation were used to calculate the mean

cemented scaled stress in all unsaturated simulations. This implies that the predicted water content is no longer constant during the tests but tends to change slightly from the initial value. This approach is, however, considered acceptable as it allows to separate the effects of cementation on mechanical behaviour, which are the focus of the present paper, from the effects of capillarity, which have already been studied in a previous publication [1].

MODEL VALIDATION

The predictive capabilities of the proposed model were assessed by simulating additional tests (i.e. tests not used during calibration) with the previously selected parameter values (Table 1). As before, these additional tests were performed on samples compacted at the same water content of 13% under slightly different loads to achieve two distinct levels of dry density equal to 1684 kg/m^3 and 1526 kg/m^3, respectively.

As during calibration, the soil suction was estimated from the experimental values of water content and void ratio by using Eq. (16b) with the parameters corresponding to each cementation level (Fig. 3). This estimated value of suction was subsequently used to calculate the mean cemented scaled stress and, hence, to predict the variation of void ratio during each test.

Fig. 8 demonstrates the good performance of the model in predicting the uncemented behaviour of the soil under saturated conditions during two loading-unloading cycles on samples compacted to dry densities of 1684 kg/m^3 (triangular markers) and 1526 kg/m^3 (circular markers), respectively. In these simulations, the parameters R and λ_c were both set equal to zero and the degree of saturation was set to one inside the expression of the mean cemented scaled stress to reflect the saturated uncemented state of the soil.

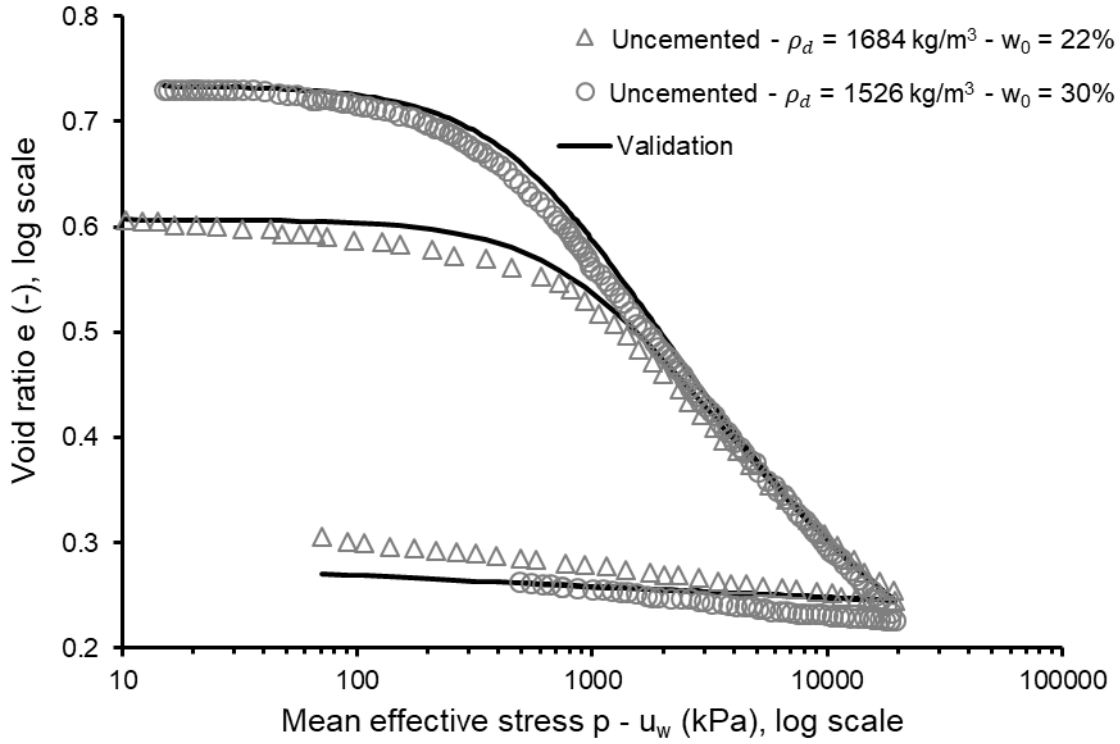

Figure 8. Prediction of the saturated uncemented behavior of samples compacted at the dry densities of 1526 kg/m^3 and 1684 kg/m^3

The ability of the model to predict the behaviour of the cemented soil under unsaturated conditions was subsequently assessed for the three cementation levels of 2%, 4% and 7%.

Fig. 9 shows the good match between the predicted and experimental behaviour of two samples compacted at a dry density of 1684 kg/m^3 with 2% of cement, which were dried to water contents of 6.7% and 11%, respectively, before being subjected to a loading-unloading cycle at constant water content. Fig. 9b also demonstrates the capability of the model to capture the transition from unsaturated to saturated states during loading [41-42].

Similarly, Fig. 10 demonstrates the ability of the model to capture the behaviour of two samples compacted at a dry density of 1526 kg/m^3 with 4% of cement by comparing predicted and experimental data for two loading-unloading cycles at constant water contents of 8.4% and 12%, respectively.

Finally, Fig. 11 compares the predicted and experimental behaviour of a sample compacted at a dry density of 1684 kg/m^3 with 7% of cement during a loading-unloading cycle at constant water content of 7.2%.

Figs. 9, 10 and 11 also show the predictions of: a) the uncemented unsaturated behaviour (dotted line) obtained by setting both parameters R and λ_c equal to zero in Eq. (6) and b) the uncemented saturated behaviour (dashed line) obtained by setting both R and λ_c equal to zero in Eq. (6) and the degree of saturation equal to one in Eq. (2). As expected, the inspection of Figs. 9, 10 and 11 indicates that the cemented soil sustains higher values of void ratio compared to the uncemented soil. This extra porosity reduces as the applied load increases due to the progressive breakage of inter-granular bonds, which causes the cemented curve to converge towards the uncemented ones. Also, the difference between cemented and uncemented curves becomes larger as the percentage of cement increases. This is due to the higher degree of cementation which enables the material to sustain a higher porosity. The model also suggests that, as the percentage of cement increases, the extra porosity sustained by capillarity tends to reduce compared to the extra porosity sustained by cementation. In other words, the contribution of capillarity to inter-granular bonding becomes less important as the degree of cementation increases, which is also consistent with previous studies [7].

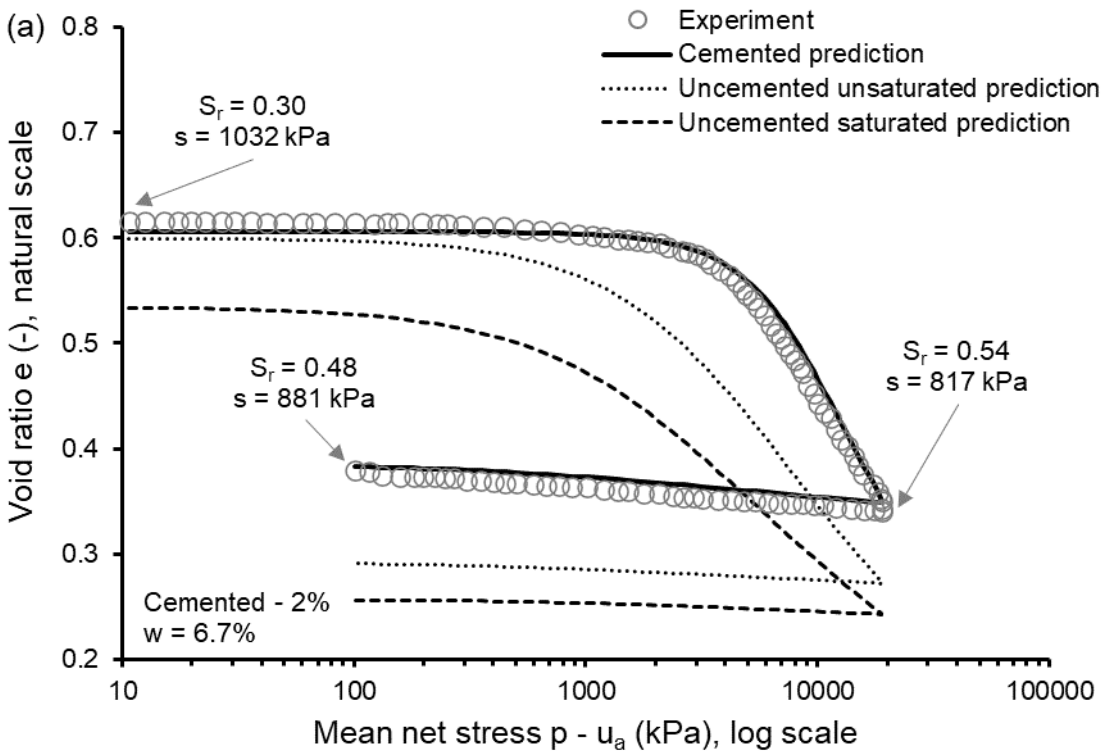

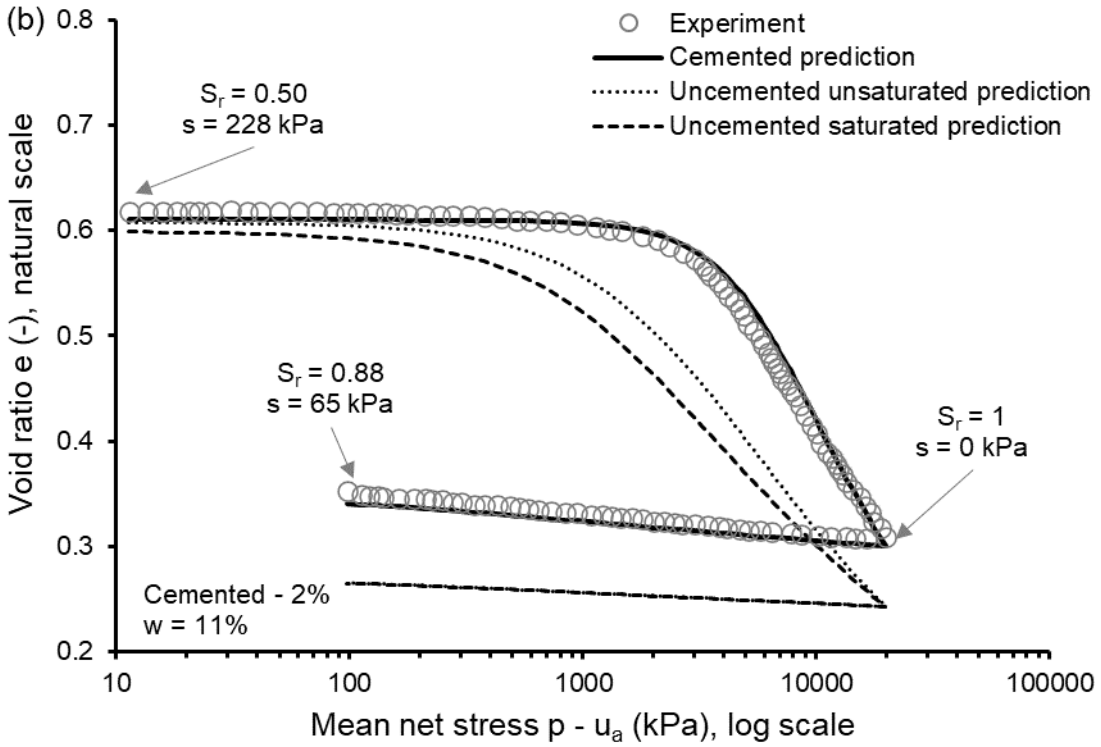

Figure 9. Prediction of cemented behavior of samples with 2% of cement tested at constant water contents of 6.7% (a) and 11% (b)

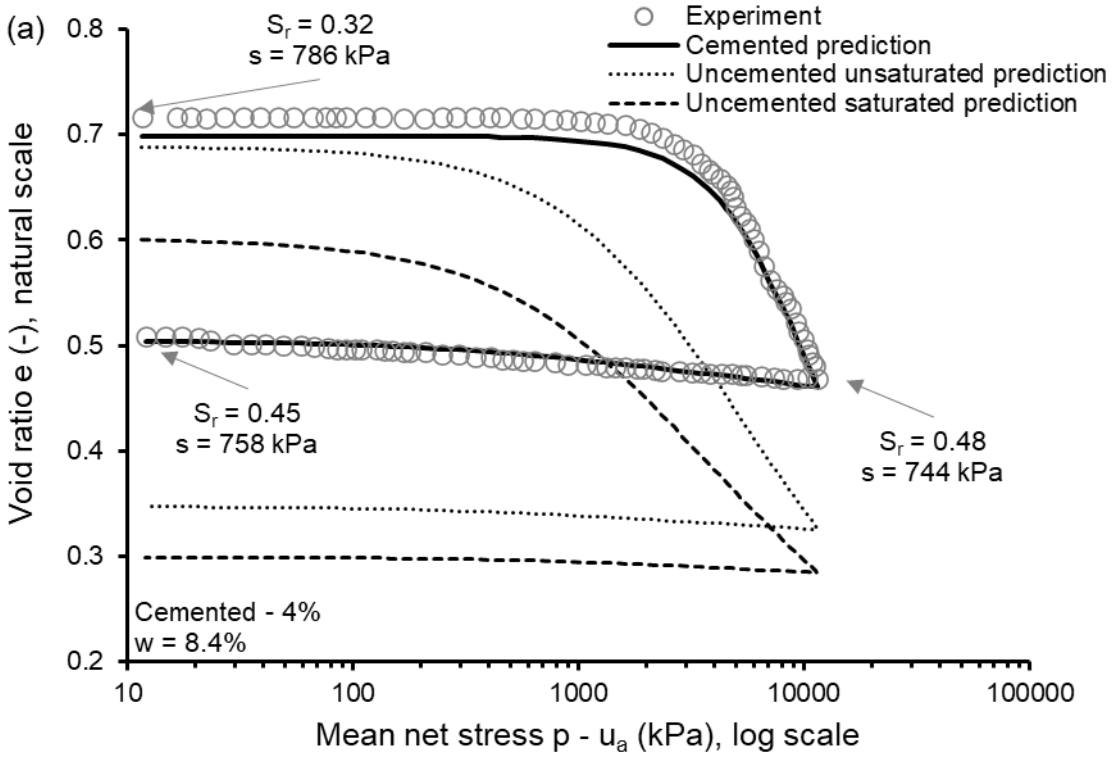

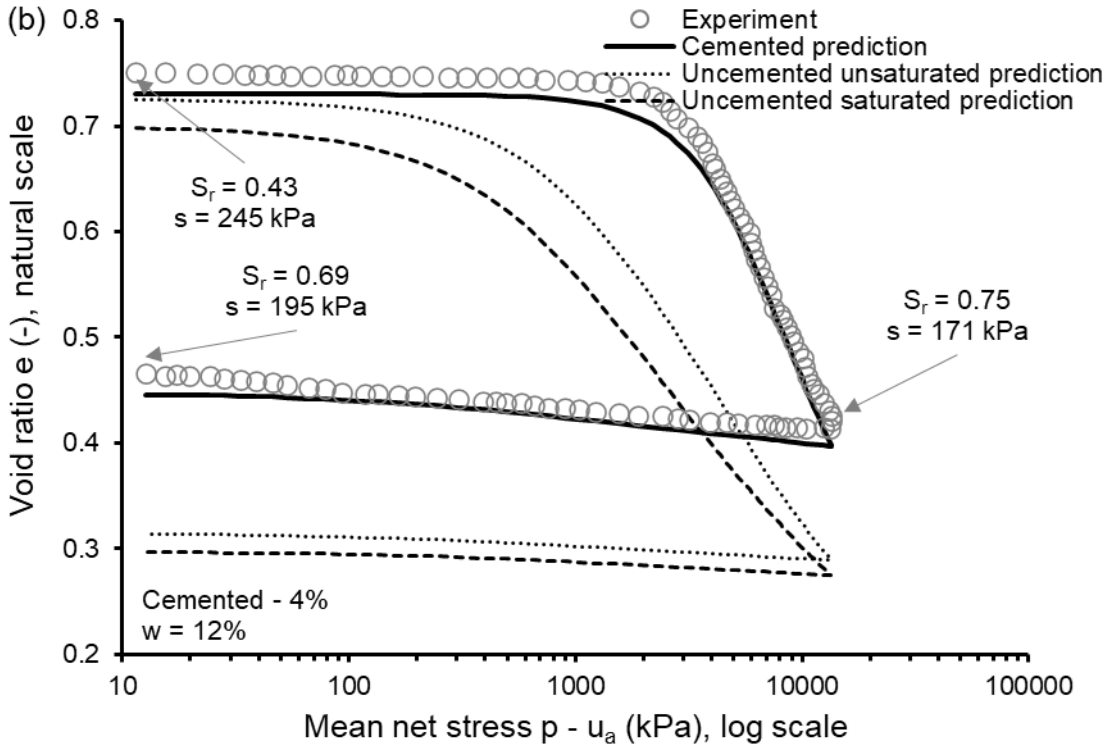

Figure 10. Prediction of cemented behavior of samples with 4% of cement tested at constant water contents of 8.4% (a) and 12% (b)

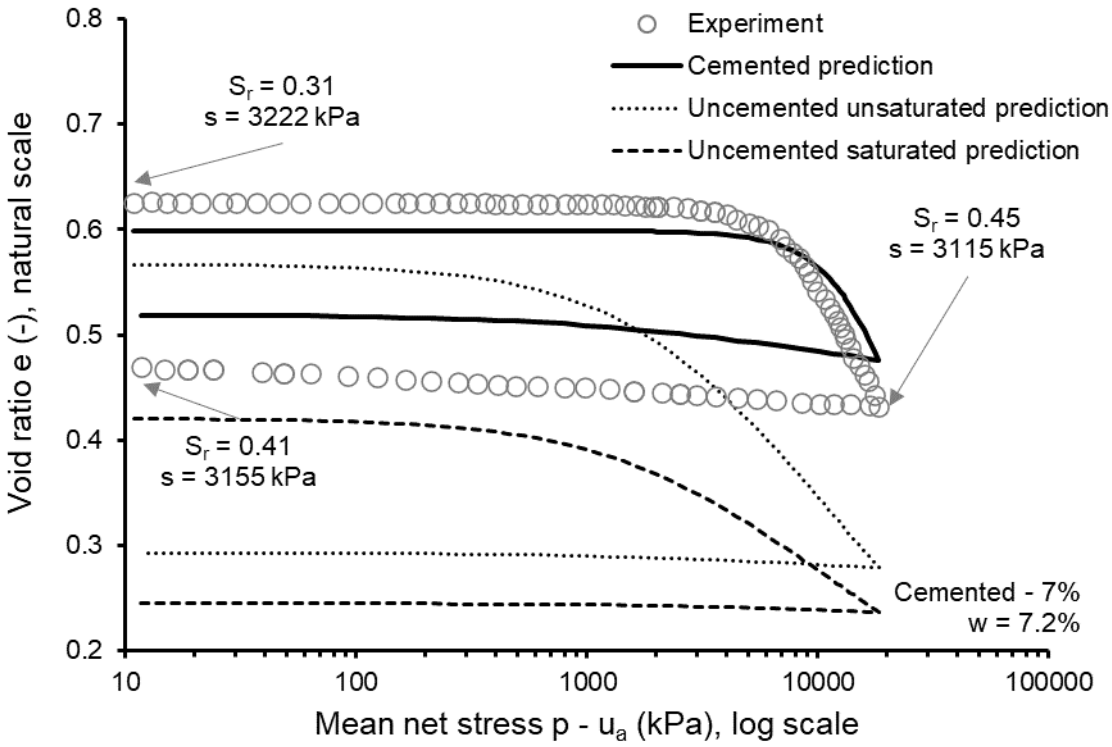

Figure 11. Prediction of cemented behavior of sample with 7% of cement tested at constant water content of 7.2%

In all validation tests, the integration constant C_L of Eq. (11) was calculated during the initial loading path by imposing that the predicted curve passes through the point defined by the experimental values of void ratio and mean cemented scaled stress after compaction [2]. These post-compaction values of void ratio and mean cemented scaled stress are slightly different from those at the beginning of the test, which explains why the predicted and experimental curves do not coincide at the onset of loading. Moreover, the same constant of integration C_L was used to predict the initial loading paths of the uncemented curves under both saturated and unsaturated conditions. This produces the observed differences between the three curves, which reflects the extra porosities sustained by capillarity and cementation, respectively. During subsequent unloading, the integration constant C_U of Eq. (14) was calculated by imposing the continuity of predictions at the reversal point for all curves, i.e. by imposing that the start of unloading coincides with the end of loading path.

As during calibration, experimental values of degree of saturation were used to calculate the mean cemented scaled stress in all simulations. This implies that the predicted water content is no longer constant during the

test but changes slightly from its initial value. This approach has, however, been taken since it has the advantage of separating the effects of cementation from those of capillarity. This is important in the validation of the proposed constitutive framework, which looks particularly at the effects of cementation on the mechanical behaviour of unsaturated soils. It is worthwhile mentioning that the developed model will facilitate the implementation of suitable soil-water retention laws, which will allow the prediction of degree of saturation and the formulation of a fully coupled hydro-mechanical model, as has been demonstrated by Bruno and Gallipoli [43] for unsaturated uncemented soils. This will also allow to study the effects of structure loss on the variation of suction and degree of saturation.

Finally, a cementation factor was defined as:

$$c = \frac{(e - e_u)}{(e - e_u)_0} \tag{17}$$

where $(e - e_u)$ is the difference between the current values of cemented and uncemented void ratio at a given mean net stress while $(e - e_u)_0$ is the difference between the cemented and uncemented void ratio at a reference mean net stress. The reference net stress state may be arbitrarily chosen, but it must correspond to a state where there is significant breakage of inter-granular cementation during loading. The cementation factor is, therefore, equal to one at the reference state but it tends to zero as the mean net stress increases causing the progressive destruction of inter-granular bonds and the consequent convergence of void ratio towards the uncemented value.

The cementation factor c defined by Eq. (17) was calculated for all the loading paths in Figs. 9, 10 and 11. For each loading path, the reference value of the mean net stress was made to coincide with the maximum difference between the cemented and uncemented void ratio predicted by the model. Table 2 summarises the maximum difference $(e - e_u)_0$ for each test and the corresponding reference values of the mean net stress $(p - u_a)_0$.

Table 2. Values of $(e - e_u)_0$ and $(p - u_a)_0$ for all loading paths

Percentage of added cement	Compaction dry density (kg/m^3)	Water content (%)	$(p - u_a)_0$ (kPa)	$(e - e_u)_0$ (-)
2%	1684	6.7	6574	0.132
		11	5063	0.134
4%	1526	8.4	5251	0.180
		12	4137	0.193
7%	1684	7.2	11755	0.221

Fig. 12 plots the variation of the cementation factor c with the ratio $\frac{p-u_a}{(p-u_a)_0}$ between current and reference values of mean net stress for all loading paths. Fig. 12 shows that, for each cementation level, samples at different water contents show similar destructuration trends. For 2% and 4% cement content, the drier samples show higher values of the reference mean net stress compared to the wetter samples (Table 2), which suggests that partial saturation affects the onset of destructuration but it has only a negligible effect on the subsequent destructuration trend. Finally, Table 2 indicates that the two samples with an intermediate cement content of 4% exhibit the lowest values of the reference mean net stress. This apparently counterintuitive finding is explained by the lower compaction density of the samples with 4% cement compared to the samples with 2% and 7% of cement (Table 2). The low value of the reference mean net stress $(p - u_a)_0$ for samples stabilised with 4% of cement also explains why the curves corresponding to this cement content exhibit , for a given cementation factor, slightly higher values of the ratio $\frac{p-u_a}{(p-u_a)_0}$ compared to the samples with 2% and 7% of cement (Figure 12).

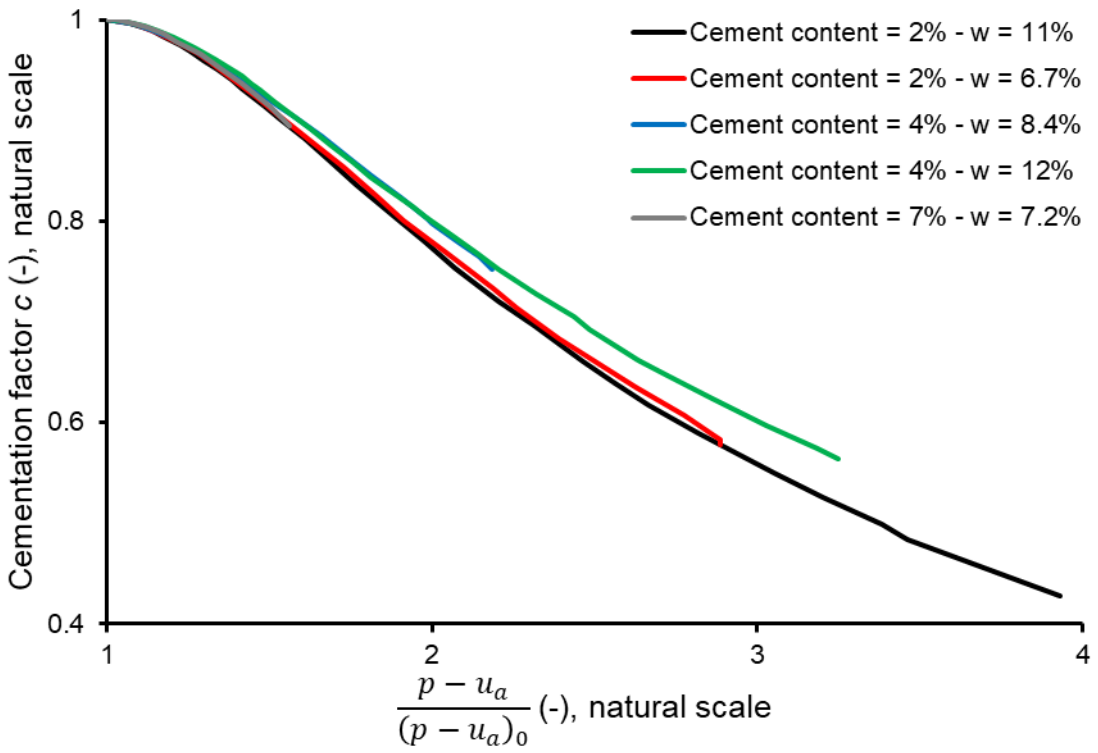

Figure 12. Variation of the cementation factor for samples with 2%, 4% and 7% of cement tested at different water contents

CONCLUSIONS

This paper has presented a bounding surface model that predicts the mechanical behaviour of unsaturated cemented soils under isotropic stress states. The model relies on the definition of a cementation bonding function that calculates the fraction between the cemented and uncemented void ratio at the same scaled stress as a monotonically decreasing function of the scaled stress. This fraction, which is always bigger than one to reflect the extra porosity sustained by cementation, decreases as the stress level increases due to the progressive breakage of inter-granular bonds. The definition of the cementing bonding function leads to the subsequent introduction of a cemented unified normal compression line (CUNCL), which is valid for both cemented and uncemented soils under unsaturated and saturated conditions. This cemented unified normal compression line is expressed in terms of a new constitutive variable named the “cemented scaled stress”,

which depends on the mean average skeleton stress and degree of saturation. The mean cemented scaled stress reduces to Terzaghi's effective stress when the soil is fully saturated and cementation is absent.

The cemented unified normal compression line delimits the region of overconsolidated soil states, where loading and unloading paths correspond to increasing and decreasing changes of the mean cemented scaled stress, respectively. The model simulates the gradual yielding of overconsolidated cemented soils by assuming that, as the stress state approaches the normal compression line, the slope of the loading path tends monotonically to the slope of the normal compression line. During unloading paths, swelling of the soil is instead modelled by assuming a linear response in the logarithmic plane of void ratio versus mean cemented scaled stress. This formulation results in the prediction of a hysteretic mechanical behaviour where each loading and unloading path is uniquely defined by a closed form mathematical expression.

The model requires a total of seven parameters to simulate the behaviour of the unsaturated cemented soil under isotropic stress states. Five of these parameters (i.e. $\lambda_p, \lambda_r, \bar{\bar{p}}_{ref}, \gamma, \kappa$) control the uncemented behaviour while two additional parameters (i.e. R and λ_c) govern the cemented behaviour. The performance of the model has been validated against a set of tests performed on both uncemented and cemented soil samples under saturated and unsaturated conditions. Results show that the proposed model is capable of accurately reproducing the mechanical behaviour of the cemented soil including the progressive transition towards the uncemented condition as loading increases. Results also show that, for a given cementation level, partial saturation influences the level of stress required to initiate breakage of inter-granular bonds, but it has only a limited effect on the subsequent destructuration. Future research will focus on the extension of the model to non-isotropic stress states and on the development of a comprehensive material framework for the coupled prediction of the mechanical and retention behaviour of unsaturated cemented soils.

REFERENCES

[1] Gallipoli, D., & Bruno, A. W. (2017). A bounding surface compression model with a unified virgin line for saturated and unsaturated soils. *Géotechnique*, 67(8), 703-712.

[2] Arroyo, M., Amaral, M. F., Romero, E., & Viana da Fonseca, A. (2013). Isotropic yielding of unsaturated cemented silty sand. *Canadian Geotechnical Journal*, 50(8), 807-819.

[3] Bertuccioli, P., & Lanzo, G. (1993). Mechanical properties of two Italian structurally complex clay soils. In *Proceedings of the International Symposium of Geotechnical Engineering of Hard Soils-Soft Rocks, Athens* (Vol. 383, p. 389).

[4] Hsu, S. C., & Nelson, P. P. (1993). Characterization of cretaceous clay-shales in North America. *Proc. Int. Sym. Geot. Eng. of Hard Soils-Soft Rocks. Anagnostopoulos et al (eds. Balkema).* Pp 139-146.

[5] Garitte, B., Vaunat, J., & Gens, A. (2006). A constitutive model that incorporates the effect of suction in cemented geological materials. In *Unsaturated Soils 2006* (pp. 1944-1955).

[6] Pinyol, P. N. M., Vaunat, J., & Alonso, E. E. (2007). A constitutive model for soft clayey rocks that includes weathering effects. *Géotechnique*, 57(2), 137-151.

[7] Pereira, J. M., Rouainia, M., & Manzanal, D. (2014). Combined effects of structure and partial saturation in natural soils. *Journal of Geo-Engineering Sciences*, 2(1-2), 3-16.

[8] Mendes, J., Toll, D.G., Augarde, C.E., & Gallipoli, D. (2008). A system for field measurement of suction using high capacity tensiometers. In *Unsaturated Soils: Advances in Geo-Engineering. Proceedings of the 1st European Conference on Unsaturated Soils, E-UNSAT 2008, Durham, United Kingdom, 2-4 July 2008* (pp. 219-225). CRC Press.

[9] Mendes, J., Gallipoli, D., Tarantino, A., & Toll, D. (2019). On the development of an ultra-high-capacity tensiometer capable of measuring water tensions to 7 MPa. *Géotechnique*, 69(6), 560-564.

[10] Gens, A. & Nova, R. (1993). Conceptual bases for a constitutive model for bonded soils and weak rocks. *Proc. Int. Sym. Geot. Eng. of Hard Soils-Soft Rocks. Anagnostopoulos et al (eds. Balkema).* Pp 485-494.

[11] Kavvadas, M., & Amorosi, A. (2000). A constitutive model for structured soils. *Géotechnique*, 50(3), 263-273.

[12] Liu, M. D., & Carter, J. P. (2000). Modelling the destructuring of soils during virgin compression. *Géotechnique*, 50(4), 479-483.

[13] Rouainia, M., & Muir Wood, D. (2000). A kinematic hardening constitutive model for natural clays with loss of structure. *Géotechnique*, 50(2), 153-164.

[14] Liu, M. D., & Carter, J. P. (2002). A structured Cam Clay model. *Canadian Geotechnical Journal*, 39(6), 1313-1332.

[15] Nova, R., Castellanza, R., & Tamagnini, C. (2003). A constitutive model for bonded geomaterials subject to mechanical and/or chemical degradation. *International Journal for Numerical and Analytical Methods in Geomechanics*, 27(9), 705-732.

[16] Vaunat, J., & Gens, A. (2003). Bond degradation and irreversible strains in soft argillaceous rock. In *Proceedings of the 12th panamerican conference on soil mechanics and geotechnical engineering*, 479-484.

[17] Baudet, B., & Stallebrass, S. (2004). A constitutive model for structured clays. *Géotechnique*, 54(4), 269-278.

[18] Carter, J. P., & Liu, M. D. (2005). Review of the structured cam clay model. In *Soil constitutive models: Evaluation, selection, and calibration* (pp. 99-132).

[19] Liu, M. D., Horpibulsuk, S., & Du, Y. J. (2015). A framework for the destructuring of clays during compression. *Geotechnical Engineering*, 46(4), 96-101.

[20] Ali Rahman, Z., Toll, D. G., & Gallipoli, D. (2018). Critical state behaviour of weakly bonded soil in drained state. *Geomechanics and Geoengineering*, 1-13.

[21] Fredlund, D. G., & Morgenstern, N. R. (1976). Constitutive relations for volume change in unsaturated soils. *Canadian Geotechnical Journal*, 13(3), 261-276.

[22] Alonso, E. E., Gens, A., & Josa, A. (1990). A constitutive model for partially saturated soils. *Géotechnique*, 40(3), 405-430.

[23] Wheeler, S. J., & Sivakumar, V. (1995). An elasto-plastic critical state framework for unsaturated soil. *Géotechnique*, 45(1), 35-53.

[24] Cui, Y.J., & Delage, P. (1996). Yielding and plastic behaviour of an unsaturated compacted silt. *Géotechnique*, 46(2), 291-311.

[25] Sun, D. A., Matsuoka, H., Yao, Y., & Ichihara, W. (2000). An elasto-plastic model for unsaturated soil in three-dimensional stresses. *Soils and foundations*, 40(3), 17-28.

[26] Loret, B., & Khalili, N. (2002). An effective stress elastic–plastic model for unsaturated porous media. *Mechanics of Materials*, 34(2), 97-116.

[27] Gallipoli, D., Gens, A., Sharma, R., & Vaunat, J. (2003). An elasto-plastic model for unsaturated soil incorporating the effects of suction and degree of saturation on mechanical behaviour. *Géotechnique*, 53(1), 123-136.

[28] Wheeler, S. J., Sharma, R.S., & Buisson, M. S. R. (2003). Coupling of hydraulic hysteresis and stress-strain behaviour in unsaturated soils. *Géotechnique*, 53(1), 41-54.

[29] Lloret-Cabot, M., Wheeler, S. J., & Sanchez, M. (2017). A unified mechanical and retention model for saturated and unsaturated soil behaviour. *Acta Geotechnica*, 12(1), 1-21.

[30] Alonso, E. E., Gens, A. (1994). On the mechanical behaviour of arid soils. Keynote Lecture in *Proc. First Int. Symp. Engineering Characteristics of Arid Soils*. London, pp. 173-205.

[31] Leroueil, S., & Barbosa, P. D. A. (2000). Combined effect of fabric, bonding and partial saturation on yielding of soils. In *Unsaturated soils for Asia. Proceedings of the Asian Conference on Unsaturated Soils, UNSAT-ASIA 2000, Singapore, 18-19 May, 2000* (pp. 527-532). AA Balkema.

[32] Yang, C., Cui, Y. J., Pereira, J. M., & Huang, M. S. (2008). A constitutive model for unsaturated cemented soils under cyclic loading. *Computers and Geotechnics*, 35(6), 853-859.

[33] Gallipoli, D., Wheeler, S. J., & Karstunen, M. (2003b). Modelling the variation of degree of saturation in a deformable unsaturated soil. *Géotechnique*, 53(1), 105-112.

[34] Gallipoli, D., Bruno, A. W., D'Onza, F., & Mancuso, C. (2015). A bounding surface hysteretic water retention model for deformable soils. *Géotechnique*, 65(10), 793-804.

[35] Hu, R., Chen, Y. F., Liu, H. H., & Zhou, C. B. (2013). A water retention curve and unsaturated hydraulic conductivity model for deformable soils: consideration of the change in pore-size distribution. *Géotechnique*, 63(16), 1389-1405.

[36] Della Vecchia, G., Dieudonné, A. C., Jommi, C., & Charlier, R. (2015). Accounting for evolving pore size distribution in water retention models for compacted clays. *International Journal for Numerical and Analytical Methods in Geomechanics*, 39(7), 702-723.

[37] Barrera, B. M. (2002). *Estudio experimental del comportamiento hidro-mecánico de suelos colapsables*. Universitat Politècnica de Catalunya.

[38] Lloret, A., Villar, M. V., Sanchez, M., Gens, A., Pintado, X., & Alonso, E. E. (2003). Mechanical behaviour of heavily compacted bentonite under high suction changes. *Géotechnique*, 53(1), 27-40.

[39] Salager, S., Nuth, M., Ferrari, A., & Laloui, L. (2013). Investigation into water retention behaviour of deformable soils. *Canadian Geotechnical Journal*, 50(2), 200-208.

[40] Gallipoli, D. (2012). A hysteretic soil-water retention model accounting for cyclic variations of suction and void ratio. *Géotechnique*, 62(7), 605-616.

[41] Lloret-Cabot, M., Wheeler, S. J., Pineda, J. A., Romero, E., & Sheng, D. (2018). From saturated to unsaturated conditions and vice versa. *Acta Geotechnica*, 13(1), 15-37.

[42] Lloret-Cabot, M., Wheeler, S.J., Pineda, J.A., Romero, E. & Sheng, D. (2018). Reply to discussion of "From saturated to saturated conditions and vice-versa". *Acta Geotechnica*, 13(2), 493-495.

[43] Bruno, A. W., & Gallipoli, D. (2019). A coupled hydromechanical bounding surface model predicting the hysteretic behaviour of unsaturated soils. *Computers and Geotechnics*, 110, 287-295.